

# Block Copolymer Formation and Synthesis of Fingerprint-Patterned AZO Nanowires for Sensor Applications

Madhurima Kundu<sup>a</sup>, Yasser Ismail<sup>a</sup> , Radian Belu<sup>a</sup> , Fred Lacy<sup>a,\*</sup> 

<sup>a</sup>Electrical Engineering Department, College of Sciences and Engineering, Southern University and A&M College, Baton Rouge, LA, USA.

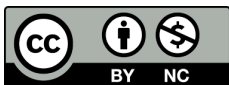
## Keywords:

Block copolymer  
Fingerprint  
Nanowires  
Infiltration synthesis

## \* Corresponding author:

Fred Lacy  
E-mail: [fred\\_lacy@subr.edu](mailto:fred_lacy@subr.edu)

Received: 12 July 2024  
Revised: 24 August 2024  
Accepted: 25 September 2024



## ABSTRACT

The study focuses on utilization of block copolymer (BCPs) as template for selective infiltration of AZO precursors. BCPs consist of chemically distinct polymer blocks that are self-assembled into well-defined domains with different morphologies. Vapor phase infiltration (VPI) provides a controlled approach for synthesizing fingerprint-patterned AZO nanowires, offering advantages in terms of conformal coating, vertical alignment, precursor control, scalability, and compatibility with atomic layer deposition (ALD) platforms making it suitable for different applications. The aim of this research is to fabricate nanostructured materials with controlled compositions and patterns which have applications in optoelectronic, sensing, surface engineering, and high-resolution imaging systems. The self-assembled structure of AZO nanowires resemble human fingerprints and exhibits a unique combination of intricate patterns, replication accuracy, large-scale reproducibility, enhanced surface area, and tailored optoelectronic properties. BCP and self-assembly allows for the accurate replication of the fingerprint pattern onto the nanowire arrays. The results demonstrate successful replication of fingerprint patterns of the AZO nanowires. Hence, based on these performance characteristics, this developed approach of fingerprint-patterned AZO nanowires represents a significant advancement in technology and hold potential for revolutionizing various fields, from security systems to sensor technologies, driving innovation in the realm of nanotechnology.

© 2025 Journal of Materials and Engineering

## 1. INTRODUCTION

The nanotechnology field has made enormous advances, controlling matter at the nanoscale [1]. The synthesis and patterning of nanowires, hold

enormous promise for applications ranging from electronics and optoelectronics to sensing and healthcare, is one area of particular interest [1]. Aluminum-doped Zinc Oxide (AZO) has received substantial interest among the numerous

materials investigated for nanowire fabrication due to its remarkable electrical and optical properties [2].

Self-assembly is based on the spontaneous organization of materials in ordered structures, which is driven by molecular interactions, whereas block copolymers is used as templates for the deposition and arrangement of nanowires [3].

The incorporation of fingerprint patterns into AZO nanowires is an intriguing research direction. This method, inspired by the distinctive ridge patterns present on human fingerprints, offers specific advantages for sensor, and optoelectronic applications.

Despite the growing interest in fingerprint-patterned AZO nanowires, there is still a need to investigate novel synthesis methods capable of accurately controlling the production and alignment of nanowires on a variety of Atomic Layer Deposition (ALD) platforms under varying conditions. Furthermore, for investigating the structural, optical, and electrical properties of these nanowires, thorough characterization techniques are required.

This thesis aims to address these gaps by investigating the synthesis of fingerprint-patterned AZO nanowires through self-assembly via Vapor Phase Infiltration (VPI) on diverse ALD platforms.

## 2. LITERATURE REVIEW

Bottom up synthesis such as Chemical Vapor Deposition (CVD) is a commonly used process that involves the chemical reactions of precursor gases on a heated substrate to generate nanowires [4]. Other bottom-up processes provide diversity and control over nanowire properties include solution-phase synthesis, hydrothermal and solvothermal procedures, and electrochemical deposition [5]. Top down synthesis such as Electron beam and focused ion beam lithography, provide fine control over nanowire geometry and location by selectively removing or depositing materials [6]. Dry etching and wet chemical etching, for example, can be used to shape and sculpt nanowires from bulk materials [7].

The CVD and VLS method have certain limitations. For requirement of pressure vaporization, adsorption and chemical reaction, the high temperatures requirement of these methods can limit the substrate materials available and may cause thermal stress during the synthesis process [8,9]. In VLS method catalyst compatibility difficulties and catalyst species diffusion can have an impact on the uniformity and quality of nanowire development [9]. Defects such as stacking faults, dislocations, and surface roughness can also be present in the nanowires, impacting their structural and electronic properties [10,11]. Vapor Phase Infiltration (VPI) is a material synthesis and functionalization approach that involves injecting vapor-phase precursors into a porous substrate or template. On the top surface of the substrate, precursors undergo chemical reactions or degrade, resulting in the creation of the desired substance or coating [12,13]. This process allows for fine control of the deposition process by altering factors such as temperature, pressure, and precursor concentration which is critical for producing the required attributes of the AZO nanowires, such as conductivity, optical qualities, and structural integrity [14].

VPI enables the deposition of AZO onto the nanowire surfaces, ensuring that the coating material and the underlying structure are compatible [15,16].

Atomic Layer Deposition (ALD) is a process to deposit thin films that is well-known for its excellent control over layer thickness, homogeneity, and conformality

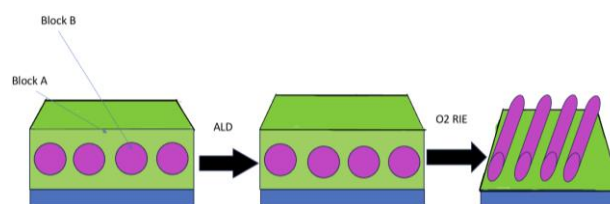


**Fig. 1.** Block copolymer formation followed by VPI and plasma ashing with O<sub>2</sub>.

ALD platforms, when paired with VPI, enable the deposition of conformal coatings on complicated patterns such as fingerprint-patterned nanowires [17]. The deposition process can be fine-tuned by modifying the parameters to produce the required coating qualities while limiting undesired side reactions or substrate damage [18].

### 3. MOTIVATION FOR THIS WORK

Aluminum-doped Zinc Oxide (AZO) is a transparent conducting oxide (TCO) which has unique qualities and characteristics such as high electrical conductivity [19], transparency in visible spectrum [20], chemically resistant in different environmental situations [19], strong thermal stability [21], good mechanical durability and adherence [21], low resistivity [20] makes it ideal for several applications.

Qingsong Xu et al. Has shown a sandwiched structure of AZO/AgNW/AZO and the synthesis method of AZO was magnetic sputtering [22]. Cheng-Liang Hsu et. Al has shown synthesizing AZO nanowires on glass substrate, and they are grown hydrothermally [23]. Jheng-Ming Huang et. al. demonstrated synthesis of ZnO nanowires by vapor phase transport process. The inner shell structures were formed from AZO films which is deposited on ZnO-NWs at 260 °C using an ALD system. AZO films are deposited with varying number of cycles [24].

The main disadvantages of these techniques are limited control over nanowire growth, complex process optimization, low throughput, high equipment cost, high pressure and temperature, contamination risk etc.

In Self-Assembly, the components try to reduce their free energy by using arrangements with lower energy states which can be accomplished using advantageous intermolecular forces such as van der Waals forces, electrostatic contacts, hydrogen bonding, or hydrophobic interactions [25]. Self-assembly frequently involves the development of supramolecular structures, in which non-covalent interactions play an important role. These reversible, weak connections enable dynamic construction and disassembly processes [26]. The system gains entropy which gains advantage to fuel the self-assembly process [27]. Self-assembly at several length scales can result in hierarchical structures [28].

When self-assembled on a substrate plane, block copolymers (BCPs) exhibit a wide range of orientations and morphologies depending on composition, molecular weight, film thickness, and interactions with the substrate. The following are descriptions of numerous orientations and morphologies seen in BCP self-assembly: Parallel

Cylinders [29], Perpendicular Cylinders[29], Parallel Lamella [29], Spheres [29].

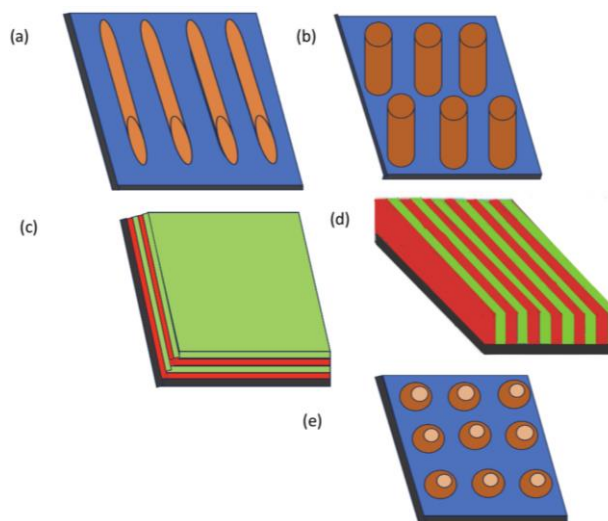


**Fig. 2.** Various orientations and morphologies of BCP domains with respect to a substrate plane obtained after self-assembly: (a) parallel cylinders, (b) perpendicular cylinders, (c) parallel lamella, (d) perpendicular lamella, and (e) spheres.

Polystyrene-*b*-poly (methyl methacrylate) (PS-*b*-PMMA) is a well-studied block copolymer (BCP) system that has several applications, nanotechnology, and surface engineering due to its unusual self-assembly characteristic. PS-*b*-PMMA is made up of two chemically different blocks, polystyrene (PS) and poly (methyl methacrylate) (PMMA), that are covalently bonded [30].

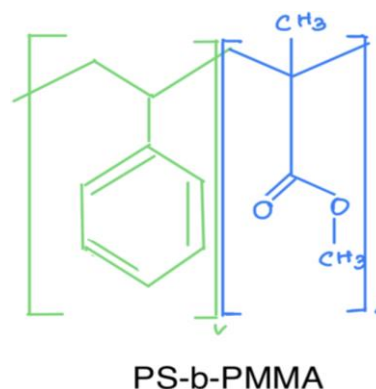


**Fig. 3.** Schematic Representation of Polystyrene-*b*-Methyl methacrylate (PS-*b*-PMMA) .

The PS block is formed of styrene monomer units and is hydrophobic, whereas the PMMA block is composed of methyl methacrylate monomer units and is hydrophilic [30]. Because of their chemical differences, the two blocks are immiscible, resulting in phase separation when the BCP is in solution or solid form. The thermodynamic goal is to decrease

interfacial energy and obtain a more favorable block segregation which drives PS-b-PMMA self-assembly [31]. The BCP works as a scaffold or guiding template, directing how the nanowires are arranged and aligned in space [32].

By altering the BCP composition, molecular weight, and processing conditions, the size and spacing of the BCP microdomains may be adjusted, providing for precise control over the nanowire characteristics [33]. For starters, it allows for the fabrication of nanowire arrays with consistent size, spacing, and orientation across wide areas, which is difficult to achieve using traditional lithographic processes [34]. Second, the BCP template enables the creation of sophisticated nanoscale patterns and architectures that would be impossible to create using other methods. Furthermore, because BCP self-assembly is scalable, it is appropriate for large-scale manufacture of nanowire-based devices and materials [34].

#### 4. MATERIALS AND METHODS

Experimental steps involve sample preparation and synthesis technique of the AZO nanowires [35]. The following procedure is used to prepare the BCP solution and prepare the sample. Fifty (50) mg/0.05 gm of P4009-SMMA (Sigma-Aldrich) (PS (47k)-b-PMMA (58k)) powder is taken. 5gm of Toluene (Sigma-Aldrich) is taken in a beaker and the powder is poured to make a solution of 1%.

The off-ratio PS:PMMA is kept 47:58 as we want a long chain formation of chain of nanowires.

The solution is to put a magnetic stirrer at 70-degree Celsius temperature with the maximum spin speed for overnight.

The brush solution is made with DOW 60 (polydimethylsiloxane) (Sigma-Aldrich) and 1% PGMEA (propylene glycol monomethyl ether acetate) (Sigma-Aldrich). The Si wafer is cut in dimension of 1.5 cm\*1.5 cm for each.

The below-mentioned recipe is the recipe for making fingerprint patterned AZO nanowires which gives a suitable result. The AlOx infiltration time is varied in different range to optimize the result more accurately. AlOx infiltration time will be varied from 50 sec to 150 sec to get a suitable range to optimize the best pattern.

Three samples are cut each of size 1.5cm\*1.5cm from SiO<sub>2</sub> coated Si wafer. Oxygen plasma RIE (March RIE, March Plasma CS1701F) cleaning is performed for 120 seconds (recipe-7, pressure: 100 mTorr, RF power: 21 Watt). RIE helps to remove any organic contaminants, particulates, oxide, polymers, and unwanted substances from the surface of the sample which will not interfere with the subsequent fabrication steps. Prepared brush solution is spin coated (Laurell WS-650-23 Spin Coater) at 3000 rpm for 30 sec at 250 °C. The spin-coated solution is annealed for 5 mins.

The sample is spin-rinsed with toluene at 3000 rpm for 30 sec to remove excess brush solution. This spin-rinsing will create thin layer of brush solution.

PS-b-PMMA solution is applied by Pasteur pipette and spin coated for the samples at the optimized spin speed 3500 rpm for 30 sec and annealed at 250 °C for 20 mins.

Infiltration Synthesis is performed in S100 Savannah ALD tool- AZO infiltration at 85 °C, exposure time for AlO<sub>x</sub> 50sec (sample1), 100 sec (sample 2), 150 sec (sample 3), 1 cycle AlO<sub>x</sub> and 6 cycles ZnO.

O<sub>2</sub> plasma RIE is performed to remove organic template for 300 sec (recipe 7, pressure: 100 mTorr, RF power: 21 Watt). Finally, the SEM inspection is performed in Scanning Transmission Electron Microscope (Hitachi 2700C).

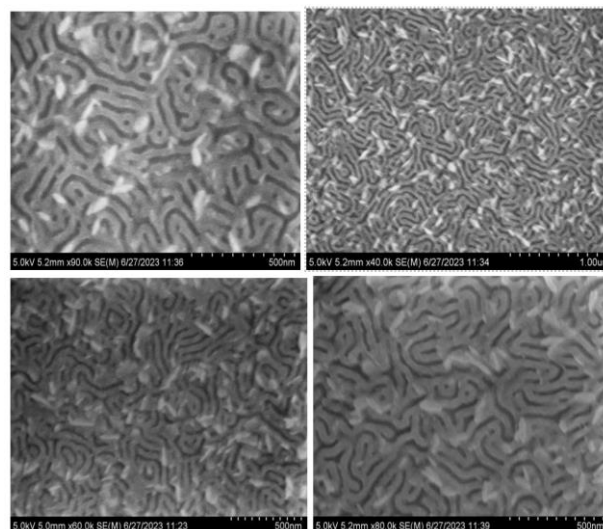
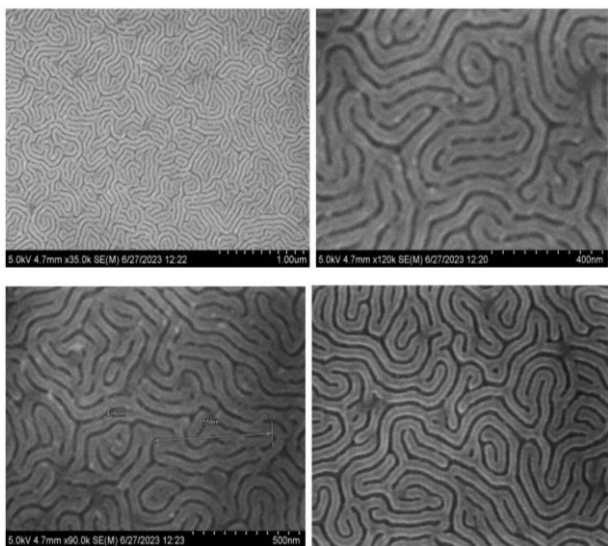


Fig. 4. AZO self-assembled fingerprint nanowires (AlO<sub>x</sub> infiltration time 50 seconds).

## 5. RESULTS AND DISCUSSION

Optical characterization (UV-Vis measurement) is performed from UV region to infrared region for all of the three samples to observe the band of wavelength of light on which the AZO nanowires are sensitive. For the reference sample SiO<sub>2</sub> coated Si wafer is taken which is the substrate used for this work. The optical characterization of reference helps to differentiate the actual sample.

The experiment was performed with the optimized parameters and in S100 ALD tool and the proper self-assembly is observed in that case. Keeping different infiltration time for AlO<sub>x</sub>, the optimized Al doping is found which is 100 seconds AlO<sub>x</sub> infiltration.



**Fig. 5.** AZO self-assembled fingerprint nanowires (AlO<sub>x</sub> infiltration time 100 seconds).

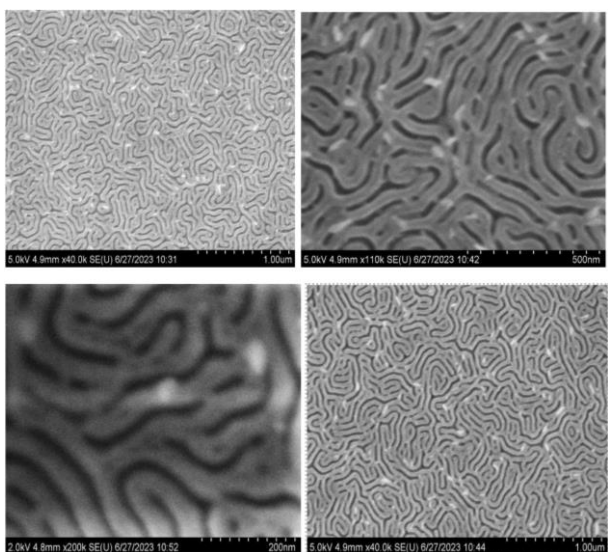


**Fig. 6.** AZO self-assembled fingerprint nanowires (AlO<sub>x</sub> infiltration time 150 seconds).

Optimizing aluminum doping was a factor for the experiment because aluminum helps to form self-assembly binding with zinc oxide. Only zinc oxide cannot create self-assembled structure because the surface reaction with PS-b-PMMA aluminum doping is required for binding with the surface. From the results it is observed that varying the aluminum infiltration time the quality of self-assembled fingerprint nanowires is changed.

Fifty (50) seconds exposures for aluminum infiltration gives the worst result. As was discussed above, aluminum helps to bind the zinc oxide to the surface. Less aluminum infiltration leads to lower quality fingerprint nanowires and in some places discontinuous patterns are observed.

For 150 seconds of aluminum infiltration, the quality of nanowire is not very good. In some random places some discontinuities are observed. 100 seconds of aluminum infiltration time gives the best self-assembled AZO fingerprint nanowire.

From UV-Vis measurement graphs it is observed that in the UV region it shows an absorption peak which is below 400 nm. Among the three samples 100 sec sample (Fig. 9) shows the maximum absorption among the three samples which is 0.25. For 50 sec sample (Fig. 8) the absorption is 0.20. For 150 sec (Fig. 10) sample the absorption is 0.18. From the optical characterization, it is concluded that 100 sec sample gives more absorption to light compared to the other two samples because 100 sec sample gave the best self-assembled structure. For 50 sec and 100 sec sample showed some discontinuities in some locations and that may degrade the absorption of light to the sample.

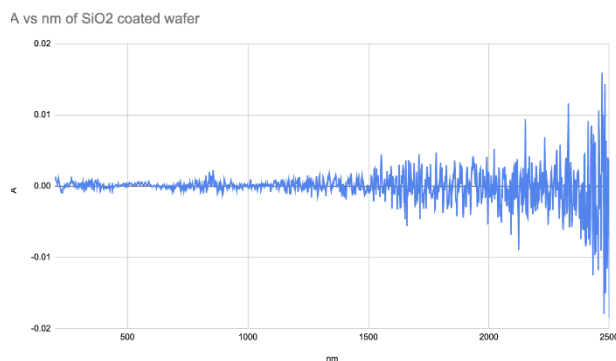


**Fig. 7.** Wavelength vs. Absorption graph for SiO<sub>2</sub> coated Si wafer.

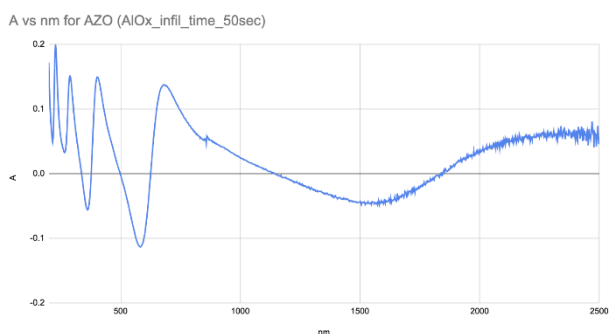


**Fig. 8.** Wavelength vs. Absorption graph of AZO nanowire (AlOx infiltration time 50 sec).

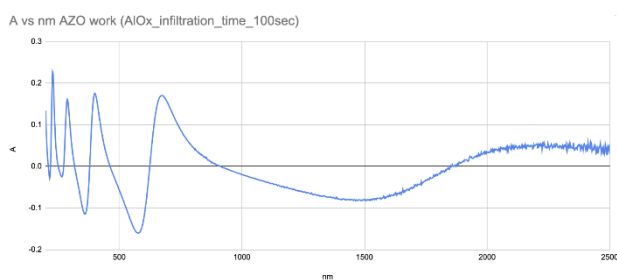


**Fig. 9.** Wavelength vs. Absorption graph of AZO nanowire (AlOx infiltration time 100 sec).

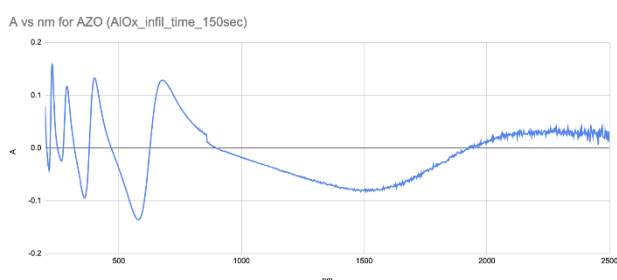


**Fig. 10.** Wavelength vs. Absorption graph of AZO nanowire (AlOx infiltration time 150 sec).

Self-assembled block copolymer (BCP) thin films have generally used as a nontraditional

material patterning process because they have the ability to spontaneously generate various nanopatterns. This process provides several advantages including reduction in material and processing cost, small feature size (<30 nm) which is not easily achievable by traditional lithographic processes, and ability to be easily incorporated into existing technology for large-scale manufacturing. The cost of photolithography ranges from \$100,000 to \$1 million. The photo mask costs several thousand dollars and the chemicals and photoresists cost a few hundred dollars per month in ongoing cost [36]. The equipment cost of electron beam lithography technique is \$500,000 to several million dollars. The consumables cost several thousand dollars [37]. For nanoimprint lithography, the equipment Cost is \$100,000 to \$500,000 for basic systems; more advanced systems can cost several million dollars. The fabrication of molds can be expensive, ranging from a few thousand to tens of thousands of dollars [38]. Extreme Ultraviolet Lithography equipments are among the most expensive lithography tools, with costs exceeding \$100 million [39].

For this work, the basic building blocks such as block copolymer, Si wafer, brush solution and other chemicals cost \$50-500 per gram. The ALD tool which is used for this work costs around \$50,000-\$70,000. The RIE tool used for this work costs approx. \$60,000. Hence from the above paragraph with the comparison of several conventional lithography techniques, this method for synthesizing the nanowires is pretty much cost-effective and scalable.

**Table 1.** Cost comparison of BCP and self assembly with traditional lithography techniques.

	Photolithography	Electron beam Lithography	Nanoimprint Lithography	Extreme UV Lithography	BCP and Self-assembly
<b>Equipment cost</b>	Very High [36]	Very High [37]	Moderate [38]	Very High [39]	Low
<b>Chemical cost</b>	High [36]	High [37]	High [38]	Very High [39]	Very low

Comparison of the processing time of this technique with the traditional lithography techniques shows Self-Assembly is less time consuming than others. Photolithography generally takes 400 minutes to 600 minutes depending on the size and complexity of the masks and exposure time [36]. Electron beam lithography generally takes 600 minutes to 1-2 days depending on the complexity of the device

[40]. Nanoimprint lithography takes 500 minutes to 700 minutes [38].

For our technique, sample preparation takes approximately 30 minutes, infiltration synthesis takes 180 minutes and post infiltration ashing takes 5 minutes. Overall, it takes 215 minutes to complete the whole process.

**Table 2** Processing time comparison of self-assembly with traditional lithography techniques.

	Photolithography	Electron beam Lithography	Nanoimprint Lithography	Extereme UV Lithography	BCP and Self-Assembly
Processing time	Moderate [36]	High [37]	Moderate [38]	Moderate [39]	Fastest

## 6. CONCLUSION AND FUTURE DIRECTION

Through this thesis research, the synthesis, characterization, and prospective applications of Fingerprint-Patterned AZO Nanowires were investigated. The thesis also presented the importance of self-assembly techniques, such as VPI, in attaining accurate alignment and arrangement of nanowires to generate the fingerprint pattern. The use of ALD platforms has been critical in managing growth parameters such as film thickness, uniformity, doping, crystallinity, and surface passivation, influencing the characteristics and performance of the nanowires.

The importance of this research resides in the unique features and benefits provided by Fingerprint-Patterned AZO Nanowires. These nanowires have improved functionality, controlled alignment, tailored optical properties, patterned surface topography, and could be used in transparent conductive films, flexible electronics, anti-reflection coatings.

In conclusion, the synthesis of Fingerprint-Patterned AZO Nanowires through self-assembly via VPI on diverse ALD platforms under varied conditions offers a unique approach for tailoring nanowire properties and achieving novel functionalities. The combination of self-assembly techniques, ALD platforms, and the fingerprint pattern opens exciting opportunities for the advancement of nanoscale devices and systems across various fields of research and application.

The creation of photodetectors employing AZO (Aluminum-doped Zinc Oxide) nanowires has enormous potential for developing optoelectronic devices in the future. Future research should concentrate on material optimization, interface engineering, device architecture exploration, nanowire integration techniques, sensitivity and spectral range enhancement, noise reduction, integration with readout electronics, environmental stability, and applications other than photodetection. It is possible to develop high-performance photodetectors with enhanced efficiency, sensitivity, and reliability for various

optoelectronic applications by fine-tuning material properties, optimizing interfaces, exploring novel device architectures, developing scalable integration methods, extending the spectral range, reducing noise, integrating with readout electronics, improving environmental stability, and investigating additional applications.

## Acknowledgment

The authors would like to thank the Electrical Engineering Department at Southern University and A&M College, Baton Rouge, USA for the great support provided in full to finalize this work. This research is supported in part by Louisiana Board of Regents and NSF EPSCoR under grant number LEQSF-EPS(2023)-LINK-140. This research used Materials Synthesis and Characterization Facility of the Center for Functional Nanomaterials (CFN), which is a U.S. Department of Energy Office of Science User Facility, at Brookhaven National Laboratory under Contract No. DE-SC0012704.

## REFERENCES

- [1] Y. Mitsuya, "Significance of micro-nanomechatronics for an information-based society," *Micro-Nanomechatronics and Human Science, 2004 and The Fourth Symposium Micro-Nanomechatronics for Information-Based Society, 2004.*, Nagoya, Japan, 2004, pp. 29-31, doi: 10.1109/MHS.2004.1421266.
- [2] AZO, "Silver nanowire stacked films deposited by RF magnetron sputtering for transparent antenna," *Surface and Coatings Technology*, 2018, pp. 95-102, doi: 10.1016/j.surfcoat.2018.12.105.
- [3] H. Feng, X. Lu, W. Wang, N.-G. Kang, and J. W. Mays, "Block Copolymers: Synthesis, Self-Assembly, and Applications," *Polymers*, vol. 9, p. 494, 2017. doi: 10.3390/polym9100494.
- [4] D. Wang and H. Dai, "Low-Temperature Synthesis of Single-Crystal Germanium Nanowires by Chemical Vapor Deposition," *Angewandte Chemie*, vol. 41, pp. 4783-4786, 2002. doi: 10.1002/anie.200290047.

- [5] K. W. Kolasinski, "Catalytic growth of nanowires: Vapor-liquid-solid, vapor-solid-solid, solution-liquid-solid, and solid-liquid-solid growth," *Solid State and Materials Science*, vol. 10, pp. 182-191, 2006. doi: 10.1016/j.cossms.2007.03.002.
- [6] K. J. Jeon, J. M. Lee, E. Lee, and W. Lee, "Individual Pd nanowire hydrogen sensors fabricated by electron-beam lithography," *Nanotechnology*, vol. 20, 2009. doi: 10.1088/0957-4484/20/13/135502.
- [7] K.-S. Im et al., "Lateral GaN nanowire prepared by using two-step TMAH wet etching and HfO<sub>2</sub> sidewall spacer," *Journal of Crystal Growth*, vol. 441, pp. 41-45, 2016. doi: 10.1016/j.jcrysgro.2016.01.038.
- [8] X. Zhang, L. Li, et al., "Bandgap engineering of Ga<sub>x</sub>Zn<sub>1-x</sub>O nanowire arrays for wavelength-tunable light-emitting diodes," *Laser and Photonics Reviews*, vol. 8, pp. 429-435, 2014. doi: 10.1002/lpor.201300172.
- [9] J. C. Harmand, G. Patriarche et al., "Analysis of vapor-liquid-solid mechanism in Au-assisted GaAs nanowire growth," *Applied Physics Letters*, vol. 87, 203101, 2005. doi: 10.1063/1.2128487.
- [10] F. Yan, Y. J. Xing, Q. L. Hang, D. P. Yu, Y. P. Wang, J. Xu, Z. H. Xi, and S. Q. Feng, "Growth of amorphous silicon nanowires via a solid-liquid-solid mechanism," *Chemical Physics Letters*, vol. 323, pp. 224-228, 2000. doi: 10.1016/S0009-2614(00)00519-4.
- [11] P.-C. Chang, Z. Fan et al., "ZnO Nanowires Synthesized by Vapor Trapping CVD Method," *Chemistry of Materials*, vol. 16, pp. 5133-5137, 2004. doi: 10.1021/cm049182c.
- [12] H. Wan and H. E. Ruda, "A study of the growth mechanism of CVD-grown ZnO nanowires," *Journal of Materials Science: Materials in Electronics*, vol. 21, pp. 1014-1019, 2010. doi: 10.1007/s10854-010-0118-7.
- [13] Vapor Phase Infiltration of Metal Oxides into Nonporous Polymers for Organic Solvent Separation Membranes, *Chemistry of Materials*, vol. 31, no. 15, pp. 5509-5518, 2019. doi: 10.1021/acs.chemmater.9b01141.
- [14] I. Azpitarte and M. Knez, "Vapor phase infiltration: From a bioinspired process to technologic application, a prospective review," *MRS Communications*, vol. 8, pp. 727-741, 2018. doi: 10.1557/mrc.2018.126.
- [15] J. W. Choi, Z. Li et al., "Patterning at the 10-nanometer length scale using a strongly segregating block copolymer thin film and vapor phase infiltration of inorganic precursors," *Nanoscale*, vol. 8, pp. 11595-11601, 2016. doi: 10.1039/C6NR01409G.
- [16] A. Subramanian, N. Tiwale, and C. Y. Nam, "Review of Recent Advances in Applications of Vapor-Phase Material Infiltration Based on Atomic Layer Deposition," *JOM*, vol. 71, pp. 185-196, 2018. doi: 10.1007/s11837-018-3141-4.
- [17] G. Pellegrino et al., "Polymeric platform for the growth of chemically anchored ZnO nanostructures by ALD," *RSC Advances*, vol. 8, pp. 521-530, 2018. doi: 10.1039/C7RA11168A.
- [18] O. J. Kilbury, K. S. Barrett et al., "Atomic layer deposition of solid lubricating coatings on particles," *Powder Technology*, vol. 221, pp. 26-35, 2012. doi: 10.1016/j.powtec.2011.12.021.
- [19] S. Benkhaya, S. M'rabet, and A. El Harfi, "Classifications, properties, recent synthesis and applications of azo dyes," *Heliyon*, vol. 6, no. 1, 2020.
- [20] H. Rau, "Spectroscopic Properties of Organic Azo Compounds," *Angewandte Chemie*, vol. 12, pp. 224-235, 1973. doi: 10.1002/anie.197302241.
- [21] K. E. Lee, M. Wang, E. J. Kim, S. H. Hahn, "Structural, electrical, and optical properties of sol-gel AZO thin films," *Current Applied Physics*, vol. 9, pp. 683-687, 2009. doi: 10.1016/j.cap.2008.06.006.
- [22] Q. Xu et al., "Flexible transparent conductive films on PET substrates with an AZO/AgNW/AZO sandwich structure," *Journal of Materials Chemistry C*, vol. 2, pp. 3750-3755, 2014. doi: 10.1039/C3TC32554G.
- [23] C. L. Hsu, D. X. Hsu, T. J. Hsueh, S. P. Chang, S. J. Chang, "Transparent gas sensor and photodetector based on Al-doped ZnO nanowires synthesized on glass substrate," *Ceramics International*, vol. 43, pp. 5434-5440, 2017. doi: 10.1016/j.ceramint.2017.01.035.
- [24] J. M. Huang et al., "Enhanced electrical properties and field emission characteristics of AZO/ZnO-nanowire core-shell structures," *Physical Chemistry Chemical Physics*, vol. 18, pp. 15251-15259, 2016. doi: 10.1039/C6CP01011C.
- [25] Y. Mai and A. Eisenberg, "Self-assembly of block copolymers," *Chemical Society Reviews*, vol. 41, pp. 5969-5985, 2012. doi: 10.1039/C2CS35115C.
- [26] J. N. L. Albert and T. H. Epps, "Self-assembly of block copolymer thin films," *Materials Today*, vol. 13, pp. 24-33, 2010. doi: 10.1016/S1369-7021(10)70106-1.
- [27] S. B. Darling, "Directing the self-assembly of block copolymers," *Progress in Polymer Science*, vol. 32, pp. 1152-1204, 2007. doi: 10.1016/j.progpolymsci.2007.05.004.

- [28] R. F. Storey and D. Baugh, "Poly (styrene-b-isobutylene-b-styrene) block copolymers and ionomers therefrom: Morphology as determined by small-angle x-ray scattering and transmission electron microscopy," *Polymer*, vol. 41, pp. 3205–3211, 2000. doi: 10.1039/C2CS35115C.
- [29] R. A. Segalman, "Patterning with block copolymer thin films," *Materials Science and Engineering: R: Reports*, vol. 48, pp. 191-226, 2005. doi: 10.1016/j.mser.2004.12.003.
- [30] L. Wan, "The Limits of Lamellae-Forming PS-b-PMMA Block Copolymers for Lithography," *ACS Nano*, vol. 9, pp. 7506–7514, 2015. doi: 10.1021/acs.nano.5b02613.
- [31] V. Gianotti, "On the Thermal Stability of PS-b-PMMA Block and P(S-r-MMA) Random Copolymers for Nanopatterning Applications," *Macromolecules*, vol. 46, pp. 8224–8234, 2013. doi: 10.1021/ma401023y.
- [32] Y. S. Jun, "Fabrication of Diverse Metallic Nanowire Arrays Based on Block Copolymer Self-Assembly," *Nano Letters*, vol. 10, pp. 3722–3726, 2010. doi: 10.1021/nl1023518.
- [33] M. Singh and A. Agrawal, "Soft-Shear-Aligned Vertically Oriented Lamellar Block Copolymers for Template-Free Sub-10 nm Patterning and Hybrid Nanostructures," *ACS Applied Materials & Interfaces*, vol. 14, pp. 12824–12835, 2022. doi: 10.1021/acsami.1c23865.
- [34] S. Park and B. Kim, "Preparation of Metallic Line Patterns from Functional Block Copolymers," *Small*, vol. 5, pp. 1343-1348, 2009. doi: 10.1002/sml.200801409.
- [35] W. I. Lee, A. Subramanian, K. Kisslinger, N. Tiwale, and C. Y. Nam, "Effects of alumina priming on the electrical properties of ZnO nanostructures derived from vapor-phase infiltration into self-assembled block copolymer thin films," *Materials Advances*, 2024.
- [36] J. R. Puryear et al., "Advanced Fabrication Technique of Microengineered Physiological System," *Micromachines*, vol. 11, no. 8, p. 730, 2020. doi: 10.3390/MI11080730.
- [37] D. J. Theon et al., "Combined Ultraviolet and Electron Beam Lithography with Microresist Technology GmbH ma N-1400 resist," *Journal of Vacuum Science & Technology B*, vol. 40, 052603, 2022. doi: 10.1116/6.0001918.
- [38] H. Choi et al., "Realization of high aspect ratio metalenses by facile nanoimprint lithography using water-soluble stamps," *Photonix*, vol. 4, p. 18, 2023. doi: 10.1186/s43074-023-00096-2.
- [39] P. Samal et al., "Direct deep UV lithography to micropattern PMMA for stem cell culture," *Material Today Bio*, vol. 22, 100779, 2023. doi: 10.1016/j.mtbio.2023.100779.
- [40] E. Sharma et al., "Evolution of Lithography Techniques: Microlithography to Nanolithography," *Nanomaterials*, vol. 12, no. 16, p. 2754, 2022. doi: 10.3390/nano12162754.